Ageing reactions in a high carat gold alloy for dental porcelain bonding

K. HISATSUNE, Y. TANAKA, K. UDOH and K. YASUDA
Department of Dental Materials Science, Nagasaki University School of Dentistry, Nagasaki 852, Japan

The phase transformation during continuous heating of a high carat gold alloy used for porcelain bonding was investigated by electrical resistivity measurements, hardness tests, X-ray diffraction and scanning and transmission electron microscopy. Four reaction stages (I, II, III and IV) were found. Stage I corresponded to the formation of a short-range order. A discontinuous precipitation took place in stage II, which contributed to remarkable hardening. Stages III and IV were reactions to the stable phases at each temperature region, and resulted in softening. The activation energies for stages I, II and III are 27.1, 33.8 and 58.2 kcal/mol, respectively.

1. Introduction

In the previous decade, many kinds of alloys have been produced for dental porcelain bonding. It is also well known that most of these alloys have been subject to some age-hardening because of small additions such as In, Sn or Fe [1]. Although hardening behaviour has been studied by many investigators, the hardening reactions have been elucidated imperfectly. With respect to palladium-based alloys, Hisatsune *et al.* [2, 3] have reported the existence of a face-centred tetragonal (fct) structure based on Pd_3In. In gold-based alloys, Smith *et al.* [4] and Fuys *et al.* [5] speculated on the precipitation of an ordered face-centred cubic (fcc) structure, $FePt_3$. German [6] reported an ordered fct structure, $PtFe_{0.6}Co_{0.3}$, as a hardening reaction product. Recently, Hisatsune *et al.* [7] reported a short-range order (SRO), a long-range order of Pd_3Sn with $L1_2$ structure, and an Ostwald ripening phenomenon in a low carat gold alloy produced for porcelain bonding. However, there is little information on phase transformation in high carat gold alloys for dental porcelain bonding.

The aim of the present study is to clarify the ageing reaction during continuous heating of a high carat gold alloy produced for dental porcelain bonding.

2. Material and methods

The alloy used in the present study is a high gold alloy with 73 wt % Au; 13.0 wt % Pt, 9.7 wt % Pd, 2.8 wt % Ag and 1.5 wt % *X* (KIK HARD II, Ishifuku Metal Industry Co. Ltd., Tokyo, Japan) produced for dental porcelain bonding. It has already been reported that the unknown element *X* was Sn [2].

Sheets of 0.5 and 0.1 mm thickness were prepared by alternate rolling and annealing. The former was used only for hardness tests. All specimens were solution-treated at 1000 °C for 30 min and then quenched into iced brine. Continuous heating was subsequently carried out at a heating rate of 0.25, 0.5, 1, 2 or 10 °C/min from room temperature to 1000 °C in vacuum. Hardness tests were performed with a Vickers micro-hardness tester using a load of 200 g. Each hardness value is computed from the average of five indentations. Electrical resistivity measurements were made using a potentiometric method [8]. Structural changes were examined with an X-ray diffractometer (XRD), and scanning and transmission electron microscopes (SEM and TEM). The electron microscopes used were an S-520 and an H-800 operating at 20 kV and 200 kV, respectively. For TEM study, 3 mm diameter discs were punched from the heat-treated sheets. They were electrothinned by a double-jet technique in a solution of 35 g of CrO_3, 200 ml of CH_3COOH and 10 ml of H_2O. XRD studies were carried out on the filed and apropriately heat-treated powder specimens using nickel-filtered CuK_α radiation.

3. Results and discussion

3.1. Electrical resistivity changes

Fig. 1A shows anisothermal annealing curves of electrical resistivity ρ at a heating rate of 0.25, 1 and 10 °C/min. To exclude errors arising from specimen size differences, a normalized resistivity ρ_T/ρ_{1000} is used in this figure. ρ_T and ρ_{1000} are the resistivities at T and 1000 °C, respectively. Although the data for heating rates of 0.5 and 2 °C/min are not plotted in Fig. 1 to avoid confusion, similar resistivity changes were observed at all heating rates. It is though that these changes may be attributed to phase transformations. The faster the heating rate, the higher the initiation temperatures of reactions. We explain the variations for the case of a heating rate of 1 °C/min (solid circles). Four abnormal initiations indicated by

0957–4530

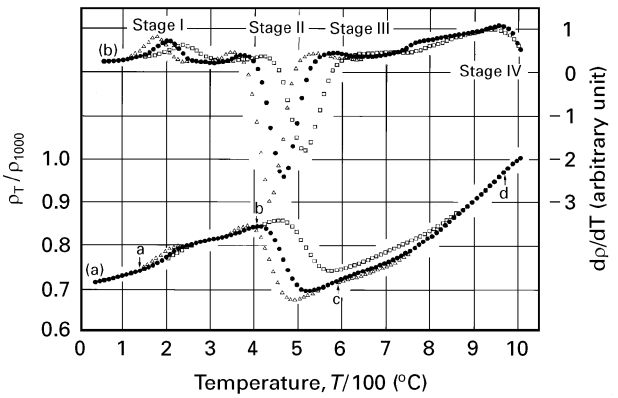

Figure 1 Anisothermal annealing curves of (a) electrical resistivity (ρ) and (b) their temperature derivatives (dρ/dT). Solution-treated at 1000 °C for 30 min. Heating rate: △ 0.25; ● 1; □ 10 °C/min.

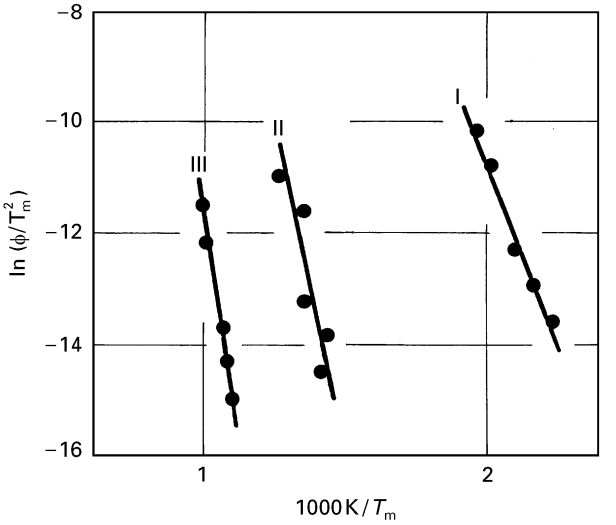

Figure 2 Kissinger plots for stages I, II and III.

arrows a, b, c and d are confirmed. These initiation temperatures are shown more clearly on the temperature derivative dρ/dT curves shown in Fig. 1B. The dρ/dT values were calculated using a least squares method with five points. Hereafter, these reactions are refered to as stages I, II, III and IV, stage I being for the lowest temperature. Stage II is the main reaction in the alloy studied.

As seen in Fig. 1, the reaction rate at each stage depends on the heating rate. The heating rate dependencies were analysed using a Kissinger method [9], the straight line Kissinger plots being as shown in Fig. 2. T_m is the temperature at which the reaction rate attained a maximum value; ϕ is the heating rate. The related plots yield apparent activation energies equal to 27.1, 33.8 and 58.2 kcal/mol for stages I, II, and III, respectively.

3.2. Age-hardening behaviour

Fig. 3 shows the variation of hardness with temperature during continuous heating at a rate of 1 °C/min. The hardness begins to increase from about 400 °C and attains a peak value at about 600 °C. Thereafter, softening occurs with increasing temperature. The temperature region 400–600 °C, which corresponds to

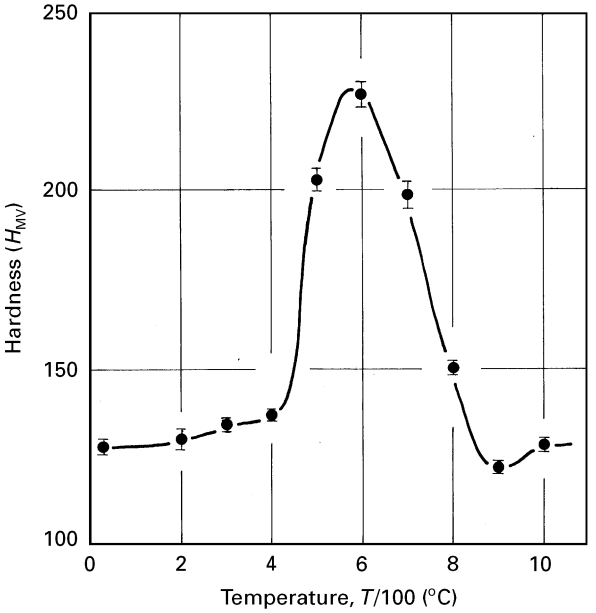

Figure 3 Variation of micro-Vickers hardness with temperature during continuous heating at a rate of 1 °C/min.

stage II, produces remarkable hardening. Comparing Fig. 3 with Fig. 1B at this temperature region, it seems that the hardness increment is proportional to the output of reaction products in stage II. On the other hand, study of the temperature region 600–800 °C indicates that the softening is related to a reaction in stage III. Stages I and IV do not appear to contribute to any hardening.

3.3. Ageing reactions

Fig. 4 shows the variation of the XRD line profile in the vicinity of 140 degrees at z theta in the alloy during continuous heating at a rate of 1 °C/min. Each spectrum was obtained as the specimen was heated to a specified temperature, then quenched. The reflection line has the highest diffraction angle obtained. The solution-treated specimen is a single phase (α_0), having an fcc structure with a lattice constant $a_{422} = 0.4029$ nm. Fig. 4b and c correspond to stage II, which produced the hardening as seen in Fig. 3. Fig. 4d, e and f correspond to stage III, which produced the softening.

In stage I, no new phase was detected by XRD. Furthermore, there was no change in the lattice constant. As can be seen in Fig. 1, stage I is accompanied by a small increase of electrical resistivity, which suggests formation of SRO, or clustering. Fig. 5 shows a selected-area electron diffraction pattern, with [1 1 0] incidence, of a specimen heated to 190 °C at a rate of 1 °C/min. The diffuse scattering due to SRO, as described by Ohshima and Watanabe [10] and Shiraishi [11] in Cu–Pd alloys, is observed near the superlattice spot positions (indicated by arrows). Shiraishi [11] has also reported a resistivity increment. According to Mott [12], the resistivity peak occurs when the SRO domains attain the size for which the scattering of electrons is a maximum. An SRO based on the Au–Pd system is anticipated from the constitutional elements, as Logie *et al.* [13] and

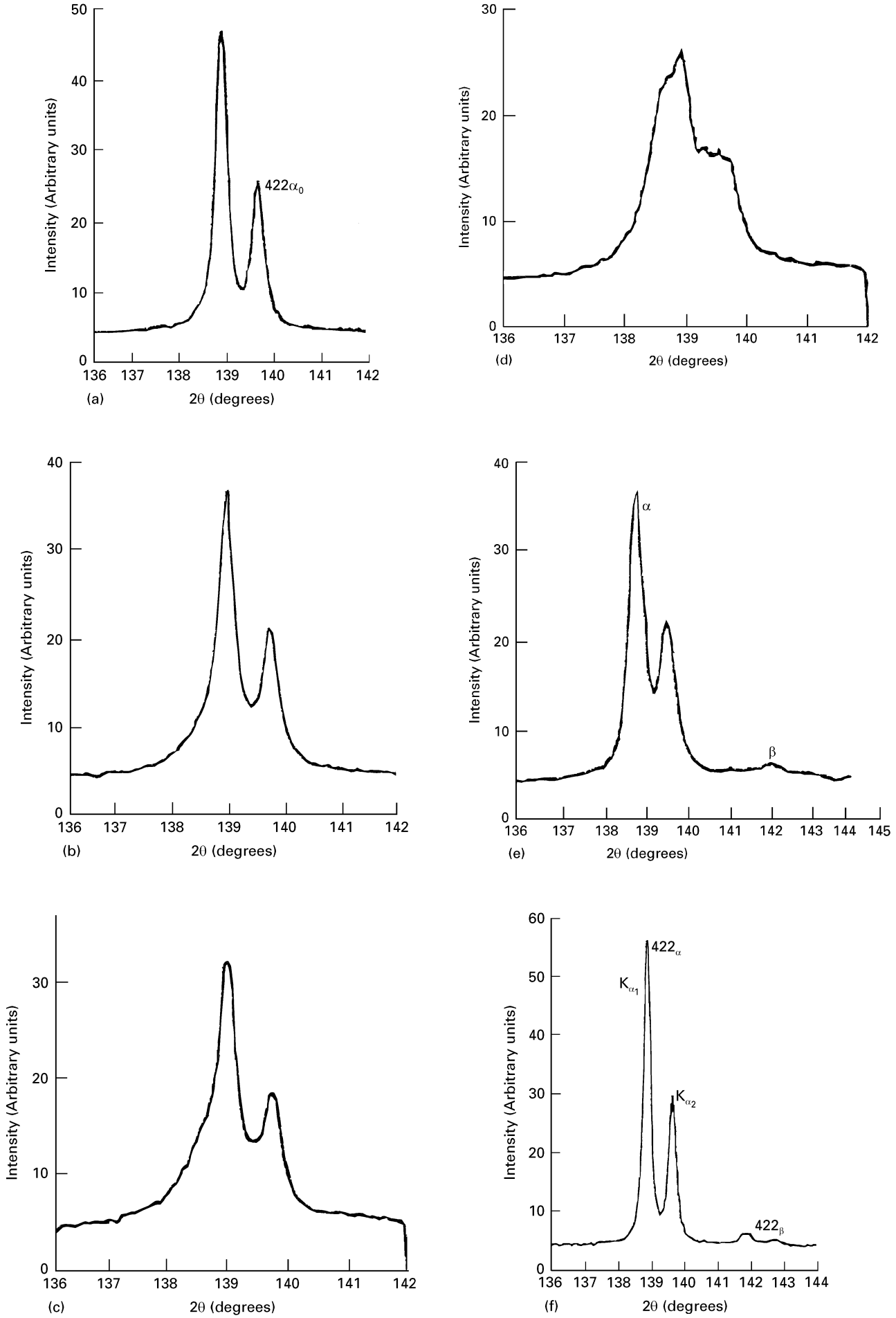

Figure 4 Variation of the XRD line profile on a reflection of 422 during continuous heating at a rate of 1 °C/min: (a) as solution-treated; and heated to (b) 500 °C, (c) 600 °C, (d) 700 °C, (e) 800 °C and (f) 900 °C, and quenched.

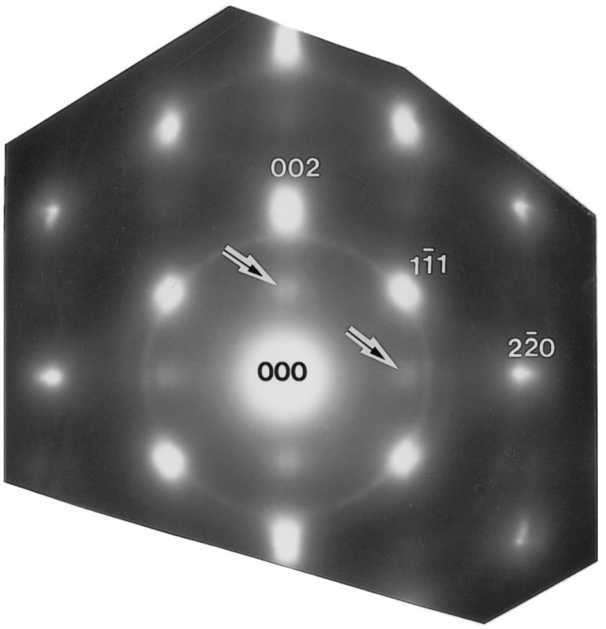

Figure 5 Selected-area electron diffraction pattern with [1 1 0] incidence of specimen annealed to 190 °C at 1 °C/min and quenched.

Copeland and Nicholson [14] have reported for binary Au–Pd alloys. The activation energy for stage I was 27.1 kcal/mol. If the migration energy of Pd is assumed to be about half of the activation energy for self-diffusion [15], Pd is reasoned to be a diffusion element. During quenching from 1000 °C after the solution treatment, excess vacancies, i.e. quenched-in vacancies, are introduced into the specimen. Subsequent annealing might be expected to produce annihilation of the excess vacancies and result in some changes of physical properties, as reported by Hisatsune *et al.* for CuPt [16] and a low carat gold alloy [7]. The value of 27.1 kcal/mol should correspond to the migration energy of quenched-in excess vacancies.

Although no new XRD reflection line in stage II was found, the foot of the 422 reflection line from matrix α_0 expands, as seen in Fig. 4b and c. It is suggested that precipitation occurs in stage II. It is considered that the original line is piled up by the broad line from a precipitate, whose lattice constant is very close to that of the matrix phase. In this stage, the reflection from matrix α_0 becomes broader and remarkable hardening was produced as can be seen in Fig. 3. Fig. 6a shows a bright-field image of the specimen heated to 400 °C at 1 °C/min. A very fine grain boundary product is observed. This is very similar to the micrograph reported by Butler *et al.* [17], which indicated the existence of convex forward grain growth. The evidence suggests that the convex forward growth proposed by Tu and Turbull [18] is favoured in the present alloy. Fig. 6d shows a selected-area electron diffraction pattern from the central region, indicated by a circle in Fig. 6a. Analysis proves that this pattern consists of [1 0 0] and [1 1 0] zones from grains I and II, respectively. Fig. 6b and c show dark-field images from $1\bar{1}1$ and 0 2 0 spots, which belong to grains II and I, respectively. It is obvious that this grain boundary product succeeds to the opposite grain on crystal orientation. Although spots from the precipitate could not be distinguished in Fig. 6(d), the dark-field images (Fig. 6b and c) from matrix spots must include the precipitate information. It is suggested that both the matrix and the precipitate have nearly equal lattice constant. This result is consistent with that of the XRD study, as seen in Fig. 4. Such a similarity in lattice parameter is very favourable for dental porcelain bonding because of the minimization of dimensional change. Fig. 7a shows an SEM image of the specimen heated to 470 °C at 1 °C/min, which corresponds to stage II. Having a very fine lammella structure with a spacing of about 0.1 μm, grain boundary products are readily observed. In the micrograph, untransformed parts can be observed. It is concluded that stage II corresponds to the formation of fine lamella from grain boundaries. Similar age-hardening by grain boundary reactions has previously been reported in Cu–Ag alloys by Kainuma and Watanabe [19], and in Co–W alloys by Dutkiewicz and Kostorz [20]. The activation energy of stage II is 33.8 kcal/mol. Considering from the component in the alloy, this value nearly equals the migration energy for Pt, 33.4 kcal/mol, reported by Polák [21]. Stage II may correspond to a reaction controlled by the migration of platinum.

As shown in Fig. 4d, e and f, stage III corresponds to a phase separation. Matrix α_0 phase remains, and seems to coexist with a precipitate phase, as seen in the specimen annealed to 700 °C (Fig. 4d). At higher temperature (800 and 900 °C), the matrix phase completely disappears, as seen in Fig. 4e and f. The shapes of the reflection 422α gradually become sharp and suggest softening, as can be seen in Fig. 3. The two phases α and β were identified as an fcc structure with $a_{422} = 0.4031$ nm and an $L1_2$ ordered fcc structure with $a_{422} = 0.3990$ nm, respectively. The latter is probably an ordered phase based on Pt_3Sn, judging from the components and the lattice constant. Fig. 7b shows an SEM image of a specimen heated to 850 °C at 1 °C/min, which corresponds to stage III. Granular products are observed, both at the grain boundaries and in the grain interiors. As mentioned above, the activation energy of stage III is 58.2 kcal/mol. This is comparable to the activation energy, 60.9 kcal/mol, for the diffusion of platinum in gold [15]. As a result of the annihilation of quenched-in excess vacancies in stages I and II, the equilibrium vacancy will play an important role for diffusion in stage III. It is certainly suggested that the migration of platinum produces the formation of the Pt_3Sn phase.

According to the XRD data seen in Fig. 4, it is obvious that stage IV corresponds to a reaction from two phases to a single phase. The critical temperature was estimated to be about 980 °C (Fig. 1). Previous work [2] reported that this temperature was about 950 °C, based on other resistivity curves with slower cooling rates. The true critical temperature of the present alloy must therefore lie between 950 and 980 °C.

The continuous heating in the present alloy can be characterized by the following reaction sequences;

$$\alpha_0(\text{fcc}) \xrightarrow{\text{stage I}} \text{SRO} \xrightarrow{\text{stage II}} \alpha' \xrightarrow{\text{stage III}} \alpha(\text{fcc}) + \beta(L1_2)$$
$$\uparrow \qquad\qquad \text{stage IV} \qquad\qquad \downarrow$$

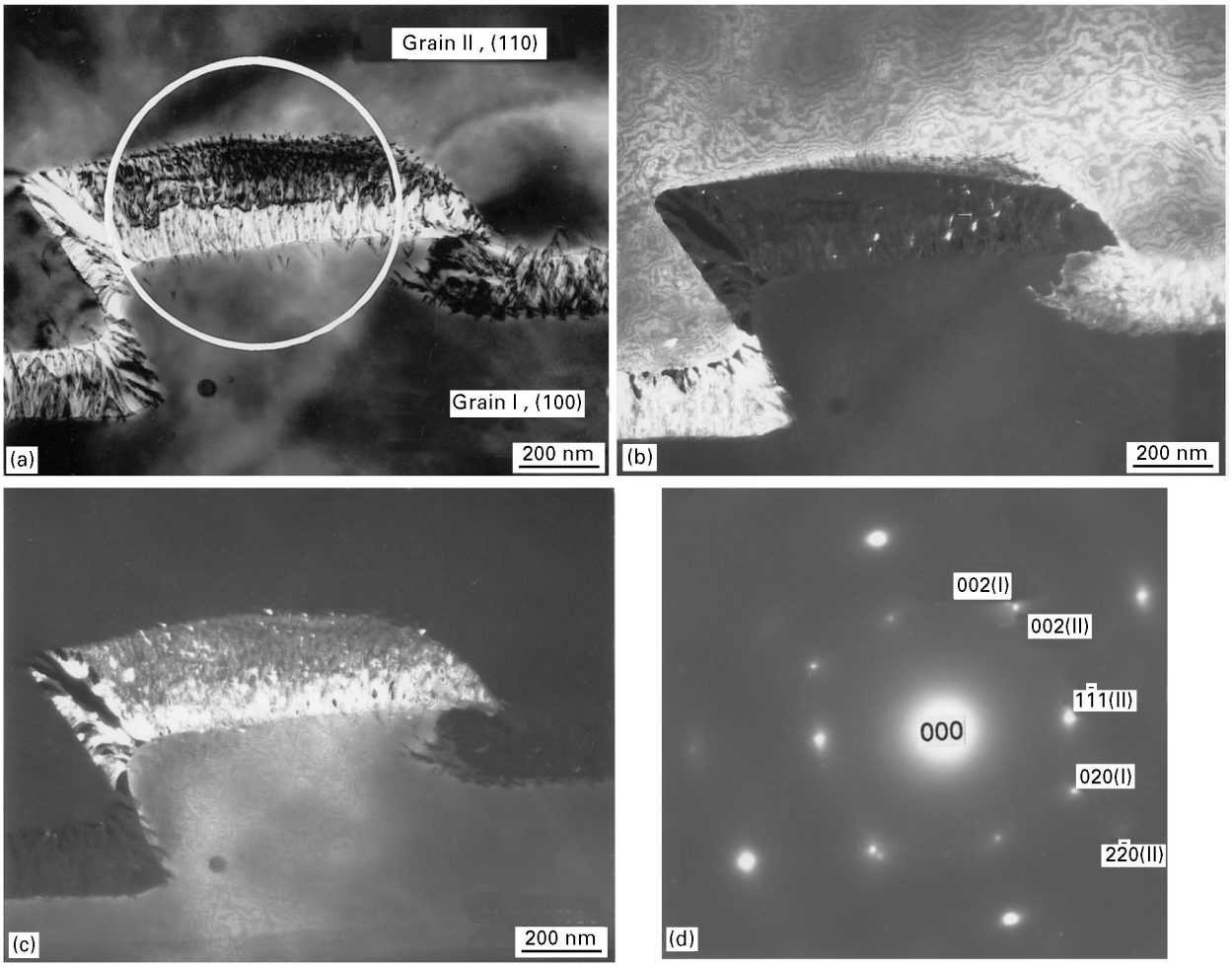

Figure 6(a) Bright-field image; (b) $1\,\bar{1}\,1_{II}$ and (c) $0\,2\,0_{I}$. Dark-field images; and corresponding selected-area electron diffraction pattern (d) of specimen annealed to 400 °C at 1 °C/min and quenched.

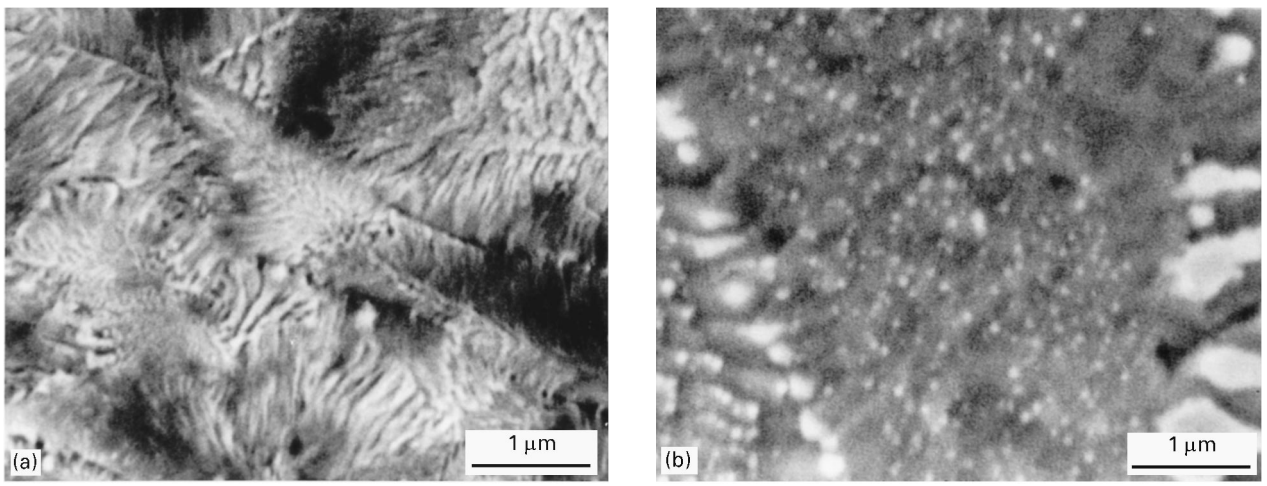

Figure 7 SEM images of the specimen heated to (a) 470 °C and (b) 850 °C at 1 °C/min.

4. Conclusions

Ageing behaviour during continuous heating of a high gold alloy for dental porcelain bonding was studied by electrical resistivity measurements, X-ray diffraction, hardness tests, scanning and transmission electron microscopies. Four reaction stages (I, II, III and IV) were found. Stage I corresponds to the formation of a short-range order. Discontinuous precipitation takes place in stage II, which contributes to hardening. Stages III and IV are reactions to the stable phases at each temperature region, and result in softening. The activation energies for stages I, II and III are 27.1, 33.8 and 58.2 kcal/mol, respectively.

Acknowledgement

This investigation was supported in part by Grant-in-Aid for Scientific Research 06671962 from the Ministry of Education, Science, Sports and Culture, Japan.

References

1. R. G. CRAIG, in "Restorative dental materials" (The CV Mosby Co., St. Louis, 1989) p. 499.
2. K. HISATSUNE, K. UDOH, M. NAKAGAWA and K. YASUDA, *Dent. Mater. J.* **6** (1987) 54.
3. K. HISATSUNE, M. HASAKA, B. I. SOSROSOEDIRDJO and K. UDOH, *Mater. Char.* **25** (1990) 177.
4. D. L. SMITH, A. P. BURNETT, M. S. BROOKS and D. H. ANTHONY, *J. Dent. Res.* **49** (1970) 283.
5. R. A. FUYS, C. W. FAIRHURS and W. J. O'BRIEN, *J. Biomed. Mater. Res.* **7** (1973) 471.
6. R. M. GERMAN, *J. Dent. Res.* **59** (1980) 1960.
7. K. HISATSUNE, Y. TANAKA, T. TANI, K. UDOH and K. YASUDA, *J. Mater. Sci.: Mater. Med.* **3** (1992) 54.
8. K. HISATSUNE, Y. TANAKA, K. UDOH, A. M. EI ARABY, K. IWANUMA and K. YASUDA, *Dent. Mater. J.* **12** (1993) 233.
9. H. E. KISSINGER, *Anal. Chem.* **29** (1957) 1702.
10. K. OHSHIMA and D. WATANABE, *Acta Crystallogr.* **A29** (1973) 520.
11. T. SHIRAISHI, PhD dissertation, Kyushu University, Japan, 1984, p. 12.
12. N. F. MOTT, *J. Inst. Metals* **60** (1937) 267.
13. H. J. LOGIE, J. JACKSON, J. C. ANDERSON and F. R. N. NABARRO, *Acta Metall.* **9** (1961) 707.
14. W. D. COPELAND and M. E. NICHOLSON, *ibid.* **12** (1964) 321.
15. Japan Institute of Metals, in "Data book for metals and alloys" (Maruzen, Tokyo, 1974) p. 24.
16. K. HISATSUNE, *J. Jpn. Inst. Metals* **42** (1978) 118.
17. E. P. BUTLER, V. RAMASWAMY and P. R. SWANN, *Acta Metall.* **21** (1973) 517.
18. K. N. TU and D. TURNBULL, *ibid.* **17** (1967) 369.
19. T. KAINUMA and R. WATANABE, *J. Jpn. Inst. Metals* **33** (1969) 198.
20. J. DUTKIEWICZ and G. KOSTORZ, *Acta Metall. Mater.* **38** (1990) 2283.
21. J. POLÁK, *Phys. Status Solidi* **21** (1967) 581.

Received 19 April
and accepted 29 May 1996